**Table 3.** Disease association or candidacy for differentially expressed genes

| Mouse gene description | AFC | | | Human homolog | | Disease |
|---|---|---|---|---|---|---|
| | P2 | P10 | 2M | Name | Location | |
| Known disease genes | | | | | | |
| Guanine nucleotide binding protein, alpha transducing 2 | 1.5 | 7.2 | 7.6 | GNAT2 | 1p13.1 | Recessive achromatopsia (ACHM4) |
| ATP-binding cassette, sub-family A (ABC1), member 4 | −1.4 | −2.8 | −2.2 | ABCA4 | 1p22.1-p21 | Recessive Stargardt (STGD1)/recessive MD/ recessive RP (RP19)/recessive fundus flavimaculatus/recessive cone-rod dystrophy |
| Cyclic nucleotide gated channel alpha 3 | — | 2.2 | 2.6 | CNGA3 | 2q11.2 | Recessive achromatopsia (ACHM2) |
| Retinal S-antigen | −5.1 | −4.1 | −1.2 | SAG | 2q37.1 | Recessive Oguchi disease / recessive RP |
| Guanine nucleotide binding protein, alpha transducing 1 | −1.2 | −55.6 | −216.4 | GNAT1 | 3p21 | Dominant congenital stationary night blindness |
| Rhodopsin | — | −24.8 | −41.3 | RHO | 3q21-24 | Dominant RP / recessive RP / dominant congenital stationary night blindness |
| Cyclic nucleotide gated channel alpha 1 | — | −7.3 | −13.6 | CNGA1 | 4p12-cen | Recessive RP |
| Prominin 1 | 1.0 | −1.9 | −1.6 | PROM1 | 4p15.33 | Recessive retinal degeneration |
| Phosphodiesterase 6B, cGMP, rod receptor, beta polypeptide | −2.3 | −37.3 | −25.0 | PDE6B | 4p16.3 | Recessive RP / dominant congenital stationary night blindness |
| Phosphodiesterase 6A, cGMP-specific, rod, alpha | — | −2.1 | −3.0 | PDE6A | 5q31.2-q34 | Recessive RP |
| Guanylate cyclase activator 1a | −1.2 | 5.6 | 1.4 | GUCA1A | 6p21.1 | Dominant cone dystrophy |
| Opsin 1 (cone pigments), short-wave-sensitive | 1.3 | 8.4 | 9.4 | OPN1SW | 7q31.3-q32 | Dominant tritanopia |
| Retinal outer segment membrane protein 1 | −2.2 | −5.3 | −3.3 | ROM1 | 11q13 | Dominant RP / digenic RP (with RDS) |
| Neural retina leucine zipper gene | — | −2.6 | −2.5 | NRL | 14q11.1-q11.2 | Dominant RP (RP27) |
| Retinoschisis 1 homolog (human) | — | −2.7 | −1.6 | RS1 | Xp22.2-p22.1 | Retinoschisis (XLRS1) |
| Candidate disease genes | | | | | | |
| S100 calcium binding protein A6 (calcyclin) | 1.1 | 1.1 | 2.1 | S100A6 | 1q21 | |
| Duffy blood group | 1.1 | 1.3 | 1.9 | FY | 1q21-q22 | Recessive cone-rod dystrophy (CORD8) |
| Retinoid X receptor gamma | −1.0 | 2.5 | 2.9 | RXRG | 1q22-q23 | |
| Adiponectin receptor 1 | −1.2 | −1.4 | −2.7 | ADIPOR1 | 1q32.1 | |
| Cytochrome b5 reductase 1 (B5R.1) | 1.1 | −1.4 | −2.0 | CYB5R1 | 1q32.1 | Recessive ataxia, posterior column with RP (AXPC1) |
| Guanylate kinase 1 | 1.0 | −1.0 | 1.9 | GUK1 | 1q32-q41 | |
| Nuclear factor of kappa light chain gene enhancer in B-cells 1, p105 | 1.1 | 1.8 | 3.1 | NFKB1 | 4q24 | Wolfram syndrome (WFS2) |
| Adenylate cyclase 2 | 1.3 | 1.9 | 2.0 | ADCY2 | 5p15.3 | Dominant macular dystrophy (MCDR3) |
| Myocyte enhancer factor 2C | – | – | −4.2 | MEF2C | 5q14 | Dominant Wagner disease (WGN1) and erosive vitreoretinopathy (ERVR) |
| 5′ nucleotidase, ecto | 1.1 | −2.1 | −2.7 | NT5E | 6q14-q21 | Recessive RP (RP25) |
| GTP binding protein (gene overexpressed in skeletal muscle) | 1.2 | 1.4 | 2.8 | GEM | 8q13-q21 | |
| Protein kinase inhibitor, alpha | 1.1 | 1.2 | 2.1 | PKIA | 8q21.11 | Recessive optic atrophy (ROA1) |
| LIM domain only 1 | −1.2 | −1.5 | −1.9 | LMO1 | 11p15 | |
| Amyloid beta (A4) precursor protein-binding, family B, member 1 | −1.0 | 1.6 | 1.9 | APBB1 | 11p15 | Dominant atrophia areata; dominant chorioretinal degeneration, helicoid (AA) |
| Cholecystokinin B receptor | 1.0 | 1.4 | 2.3 | CCKBR | 11p15.4 | |
| Muscle glycogen phosphorylase | — | 1.2 | 4.3 | PYGM | 11q13.1 | |
| Microtubule-associated protein 6 | −1.1 | 1.5 | 3.0 | MAP6* | 11q13.3 | Dominant neovascular inflammatory vitreoretinopathy (VRNI) |
| Suppressor of $K^+$ transport defect 3 | 1.0 | 2.2 | 2.2 | SKD3 | 11q13.3 | |
| RIKEN cDNA 1110002B05 gene | 1.2 | 2.3 | 2.4 | C14orf147* | 14q13.1 | Dominant MD, North Carolina-like with progressive sensorineural hearing loss (MCDR4) recessive rod monochromacy or achromatopsia (ACHM1) |
| Purine-nucleoside phosphorylase | 1.5 | 3.0 | 4.2 | NP | 14q13.1 | |
| Cerebellar degeneration-related 2 | −1.1 | −3.0 | −5.5 | CDR2 | 16p12.3 | Recessive RP (RP22) |
| Recoverin | — | −2.4 | −2.1 | RCV1 | 17p13.1 | |
| Double C2, beta | −1.0 | −1.0 | 2.0 | DOC2B | 17p13.3 | Dominant central areolar choroidal dystrophy (CACD) |
| Polymerase (DNA directed), gamma 2, accessory subunit | −1.0 | −1.7 | −3.6 | POLG2 | 17q | |
| Guanine nucleotide binding protein, gamma transducing activity pp 2 | 1.1 | 6.2 | 7.9 | GNGT2 | 17q21 | Cone rod dystrophy (CORD4) |
| Suppressor of cytokine signaling 3 | 1.1 | 1.6 | 2.4 | SOCS3 | 17q25.3 | |

Differentially expressed genes that are known to be associated with retinal diseases or candidate genes that map to disease intervals are shown. AFC is shown as given in Table 1. *Indicates that gene is the likely human homolog but is not, as yet, definitively assigned as such (based on LocusLink).

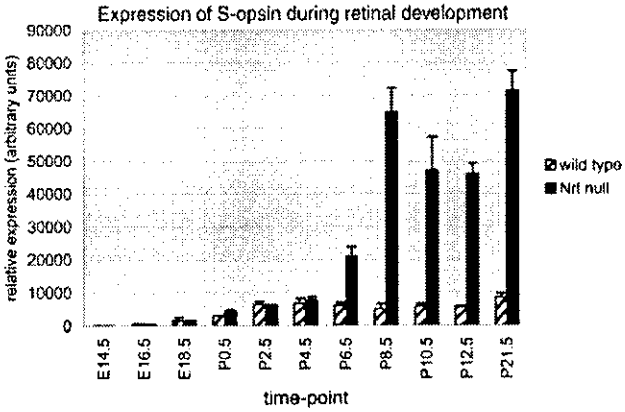


**Figure 3.** Temporal expression of S-opsin in the wild-type and $Nrl^{-/-}$ retina. The profile of relative expression of S-opsin determined by Q-PCR on the developing mouse retinas is shown after normalization to Hprt. Error bars indicate s.e.m.

observed for N-myc downstream regulated 1 (Ndr1) and Ndr-like (Ndrl).

A number of genes encoding transcription regulatory proteins are up-regulated in the $Nrl^{-/-}$ retina. Retinoid X receptor gamma (Rxrg), localized to cones in the adult retina (40) and shown to be induced by retinoic acid (RA) (41), shows 9-fold higher expression in the $Nrl^{-/-}$ retina. Rxrg maps to the region of cone-dystrophy locus CORD8 (Table 3) and is an excellent candidate for this disease. Sal-like 3 (Sall3), a C2H2 zinc finger transcription factor, is required for terminal differentiation of photoreceptors in *Drosophila* (42); its augmented expression is therefore of considerable interest. Validation by Q-PCR, which detects two of the six alternative transcripts, reveals that Sall3 is highly differentially expressed at P10 (20-fold) but is only moderately increased at 2 months (2-fold), suggesting a potential role in cone differentiation. Engrailed-2 (En2), a homeobox transcription factor, shows sustained expression in the mature wild-type retina but in $Nrl^{-/-}$ retina it is highly elevated (30-fold increase). The positive regulatory domain zinc finger protein, Prdm1, shows elevated expression (8-fold) in the matured $Nrl^{-/-}$ retina. It is expressed earlier in the wild-type retina and is undetectable in the adult.

### Apoptosis and stress response

Several genes encoding proteins associated with stress response or apoptosis exhibit decreased expression in the $Nrl^{-/-}$ retina; these include the chaperone heat shock proteins Hsp70.3 (Hspa1a) and Hsp70.1 (Hspa1b). Serum/glucocorticoid regulated kinase (Sgk), which shows peak expression in the adult retina and is down-regulated in the $Nrl^{-/-}$ retina, is shown to be anti-apoptotic and induced in response to multiple forms of stress in epithelial cells (43). Tumor necrosis factor alpha induced protein 3 (Tnfaip3), which inhibits NF-kappa B (Nfkb1) (44), has been associated with light-induced photoreceptor degeneration (45). Tnfaip3 is first detected at P10, and its expression peaks at 2 months. In contrast, Nfkb1 expression is relatively constant in the wild-type retina but exhibits a moderate peak at P2. In the $Nrl^{-/-}$ retina, Tnfaip3 is down-regulated 8-fold, whereas its inhibitory target, Nfkb1, is up-regulated. This observation, may at least in part, provide clues to the mechanism through which stress response and cell death may be mediated in the $Nrl^{-/-}$ retina during late stages (unpublished data). Caspase-7, which is detected in the wild-type retina during development, is the only caspase showing elevated (10-fold) expression in the adult $Nrl^{-/-}$ retina.

### Calcium homeostasis and retinal function

During the recovery of light response in photoreceptors, cGMP is regulated by cytoplasmic $Ca^{2+}$ via Guca1a (or Gcap1). Both Guca1a and rod arrestin (Sag) are associated with retinal diseases and are expressed differentially in the $Nrl^{-/-}$ retina. Calcium/calmodulin-dependent kinase II beta (Camk2b) is up-regulated (15-fold) in the $Nrl^{-/-}$ retina. Calcyclin (S100a6) is expressed highly in neurons (46) and shows elevated levels in the $Nrl^{-/-}$ retina. The human homolog of this gene maps to a cone–rod dystrophy locus (CORD8). S100a6 is regulated by NF-kappaB (47), which is also augmented in the $Nrl^{-/-}$ retina. Two calcium channels genes *Trpc1* and *Cacnb2* are down-regulated in the $Nrl^{-/-}$ retina. Syntrophin acidic 1 (Snta1) is a component of the dystrophin glycoprotein complex (DGC) which may play a significant structural and signaling role (neurotransmission) in the retina (48). Mutations of dystrophin or disruption of the DGC may account for scotopic (rod response) defects in patients with Duchenne muscular dystrophy (49), consistent with rod-enrichment of Snta1 and its down-regulation in the $Nrl^{-/-}$ retina.

*Melatonin signaling.* Retinal melatonin, acts as a local neuromodulator through the melatonin receptors, which then may control the release of dopamine (50). Three genes of the melatonin pathway, tryptophan hydroxylase (Tph1), dopamine receptor 4 (Drd4) and melatonin receptor 1a (Mtnr1a), are expressed differentially in the $Nrl^{-/-}$ retina. Tph1 is the first enzyme in the biosynthetic pathways of melatonin in the photoreceptors and is believed to be synthesized primarily in the cones (51), consistent with its up-regulation in the $Nrl^{-/-}$ retina. The melatonin receptor 1a, which normally shows peak expression around P2–P4, is highly elevated in the $Nrl^{-/-}$ retina, and peaks at P8 before rapidly decreasing in expression. The dopamine receptor Drd4, which plays a role in regulating cAMP metabolism, is not highly expressed until P10–P12 in the wild-type retina (52), but is down-regulated to $<10\%$ of the wild-type levels in the P10 $Nrl^{-/-}$ retina, indicating a role in rods.

### Novel functions and novel genes

Although a majority of the differentially expressed genes have a defined function, in many cases their specific role in the retina or their possible bias towards rods or cones is not understood. Deleted in polyposis 1-like 1 (*Dpl1l*) is the top FDRCI ranked down-regulated gene and is expressed at $<3\%$ of the wild-type levels. It shows peak expression in the adult retina and is detected in the outer nuclear layer (data not shown) but its function is unknown. A function can be inferred but

is not known for calcium activated chloride channel 3 (Clca3), which is up-regulated 44-fold in the $Nrl^{-/-}$ retina. Kibra is a novel WW-domain containing protein expressed primarily in brain and kidney (53) and is up-regulated 26-fold in the $Nrl^{-/-}$ retina. In addition, 18 of the differentially expressed genes identified by microarray analysis match only ESTs. These novel genes could provide new leads for elucidating retinal development and function.

## DISCUSSION

### Expression profiling and data mining

Appropriate microarray design and data analysis are essential for extracting meaningful results in genome-wide expression profiling studies (54). We utilized RMA for normalization (29,32) and chose an AFC cut-off of 1.5. A new two-stage gene filtering procedure (55) was applied that controls both FDR and minfc levels. This procedure is based on construction of a set of simultaneous FDRCI on the temporal fold-changes of each gene. Genes having at least one confidence interval that covers a range of fold-changes larger than the specified AFC cut-off, which we call minfc, are declared significant at the specified FDRCI level. As FDRCI is more stringent than FDR, the associated significance levels are generally not as high as those of the FDR procedure. For each minfc level studied, the two-stage procedure was used to generate a list of genes ranked according to decreasing FDRCI significance or, equivalently, increasing FDRCI *P*-value. For an AFC cut-off of 1.5, the complete ranked list, excluding probesets having FDRCI *P*-values >0.99, consisted of 173 probesets. Of the 54 data points tested by Q-PCR, 51 (94%) were verified. If the minfc is reduced to 1.25, the probeset list is expanded to over 300 probesets (see Supplementary Material, Table A). These additional genes may display a reduced validation rate by Q-PCR but add to cluster analysis and pathway construction based on the microarray data. Replicate experiments and statistical analysis are critical for extracting such probesets.

Temporal profiling and clustering analysis add a new dimension for predicting the functional role, possible interactions and regulatory relationships that may exist amongst the genes that are being analyzed. Our studies should identify the genes that are presumably associated with photoreceptor development (P2), terminal differentiation (P10) and function (2 month). Although our data are based on a mixed cell population (whole retina), the generated profiles are dominated by photoreceptors (about 70% of total cells) and can direct future studies to prioritize candidate genes of interest for positional cloning or functional analysis. Of particular interest are the differentially expressed genes encoding proteins associated with visual process, transcriptional regulation, signal transduction and development, as they may provide insights into the regulatory networks and signaling pathways underlying the differences between rods and cones.

Genes encoding metabolism-related proteins represented the single largest class of differentially expressed genes (24%) in the $Nrl^{-/-}$ retina. In addition, one-third of the genes are associated with light response/vision (11%), signaling (18%) and transcription (6%). There was no significant difference between up- and down-regulated genes in terms of the specific biological processes affected; however, more genes associated with vision or cell adhesion are down-regulated in the $Nrl^{-/-}$ retina (Fig. 4). This can be attributed to greater representation of rod- rather than cone-specific transcripts on the MGU74Av2 Chips. A decreased expression of genes encoding structural proteins may reflect the abnormalities of the retinal organization in the $Nrl^{-/-}$ mouse. It should be noted that cones contain more mitochondria when compared with rods (56,57); expression changes in mitochondria associated genes (*Aqp1*, *Mscs*, *Skd3* and *Clic4*) may therefore reflect numerical and physiological differences between the populations of mitochondria in the two classes of photoreceptors.

### Expanding the data set: MOE430 GeneChips and custom cDNA arrays

The MGU74Av2 GeneChip contains over 12 000 known genes and ESTs but the retina-specific transcripts are represented poorly. For example, neither Nr2e3 or cone arrestin are on these arrays. Affymetrix has since significantly improved the mouse arrays and the new MOE430 GeneChips now comprise over 36 000 genes and ESTs. These arrays are superior in design showing greater sensitivity and improved specificity of probesets. One problem with GeneChips is that the probesets are based on public databases and if transcripts are exclusively or predominantly expressed in the retina, they may not have been identified. Custom retinal cDNA arrays (28,58–60) should therefore complement GeneChip-based analysis of the $Nrl^{-/-}$ retina (J. Yu and A. Swaroop, unpublished data).

### Differential expression and reactive gliosis in the $Nrl^{-/-}$ retina

The ready-extraction of rod- or cone-specific genes from the microarray analysis is complicated by the fact that the $Nrl^{-/-}$ retina undergoes a slow form of retinal degeneration (after 4–6 months, unpublished data). A marker of retinal stress, glial fibrillary acidic protein (Gfap), is up-regulated in the $Nrl^{-/-}$ retina (18). Reactive gliosis or glial hypertrophy is observed as part of the complex neuronal remodeling that occurs during retinal degeneration (61,62). Discrimination between photoreceptor-based differential expression and changes due to retinal remodeling must be evaluated carefully, especially when dealing with genes that encode proteins with a poorly defined function. One experimental strategy would be to compare gene profiles, reported here, to those of mouse models of retinal degeneration.

### Cones or 'cods'

In the original characterization of the $Nrl^{-/-}$ mouse, the photoreceptor population was referred to as 'cods' as there was uncertainty as to whether the later developing but functional cones were in fact a type of hybrid photoreceptor. Subsequent analysis with cone-specific markers (such as PNA), suction electrode recordings of isolated photoreceptors (S.S. Nikonov, L. Daniele, A.J. Mears, A. Swaroop and E.N. Pugh Jr, unpublished data) and ERG of whole retina, nuclear

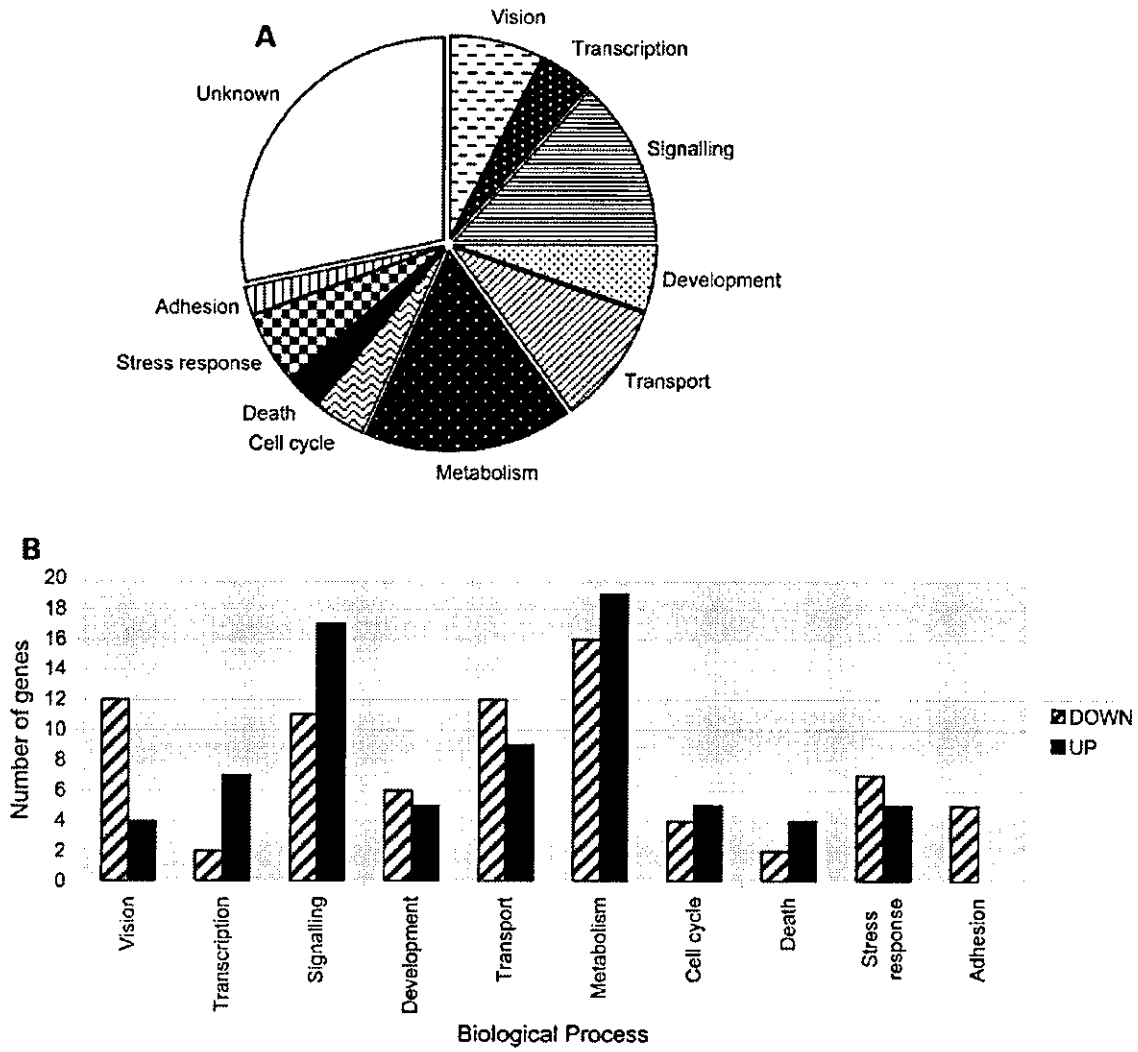


**Figure 4.** Biological processes associated with differentially expressed genes. (**A**) Overall distribution of all differentially expressed genes, (**B**) a comparison between up- and down-regulated genes.

morphology of the ONL (punctate staining typical of cones) and extensive molecular studies are all consistent with these photoreceptors being cones. Histologically, the retina is abnormal with rosettes and whorls disrupting the ONL, and short, sparse and disorganized OS. These changes, however, may be a consequence of inappropriate nuclear and OS packing within ONL and the sub-retinal region, and may be secondary to the actual identity and differentiation of the photoreceptors. The gene profiling data, presented here, provide strong evidence in favor of the photoreceptors of the $Nrl^{-/-}$ retina being cones and not cods.

### Photoreceptor plasticity and identity

In the absence of Nrl, the failure of the retinal photoreceptors to adopt their appropriate rod identity results in their transformation into cones primarily expressing S-opsin (S-cones). Nrl therefore appears to act as a molecular switch during photoreceptor differentiation by promoting the rod differentiation program while simultaneously repressing the cone identity. The suppression of the cone fate is achieved, at least in part, through direct or indirect regulation of the transcription factor Nr2e3 (20,21), whose expression is undetectable in the $Nrl^{-/-}$ retina (18).

How does Nrl orchestrate the coordinated expression of a broad array of genes that are required for making a mature and functional rod? Delineation of direct downstream targets is the essential first step towards assembling the Nrl-mediated transcriptional regulatory network(s) underlying rod differentiation. Our study has identified several potential direct targets of Nrl by a combined approach of microarray profiling and ChIP. Several of these are known or putative transcription factors or signaling proteins that may play a role in rod or cone

differentiation. Comparative retinal gene profiling studies of mouse loss-of-function mutants of other photoreceptor transcription factors (e.g. Crx, Trβ2, Nr2e3) should provide considerable insights into the gene regulatory networks that govern differentiation and homeostasis.

## MATERIALS AND METHODS

### Animal use and tissue collection

University Committee on Use and Care of Animals of the University of Michigan approved all procedures involving mice. Both the $Nrl^{-/-}$ mice and the wild-type controls were of a matched mixed genetic background (R1 and C57BL/6 strains) (18). Mice were sacrificed by cervical dislocation, and the retinas were excised rapidly, frozen on dry ice and stored at −80°C. No signs of pathology were detected in any of the animals used. To isolate sufficient total RNA for labeling protocols, retinas from two mice were pooled into a single sample. To minimize false positives due to biological variation, different samples were utilized for four replicate experiments per genotype/time-point (biological replicates). For the developmental Q-PCR studies, retinas were dissected from the embryos of timed-pregnant $Nrl^{-/-}$ or wild-type females and pooled. Retinas from post-natal time-points were also pooled (entire litter) after dissection.

### RNA preparation

Tissues were placed into TRIzol (Invitrogen, Carlsbad, CA, USA) (added to the frozen tissues at ~1.3 ml per four retinas) and homogenized (Polytron, Kinematica, Lucerne, Switzerland) at maximum speed for 120 s. Subsequent steps were done according to the manufacturer's instructions.

### Gene expression analysis

The GeneChips (Affymetrix, Santa Clara, CA, USA) used in the study contained ~12 000 probe sets, corresponding to over 6000 genes and 6000 ESTs (Murine Genome U74A Array v2).

Total retinal RNA was used to generate double-stranded cDNA (ds-cDNA) with SuperScript Choice System (Invitrogen) and oligo-dT primer containing a T7 RNA polymerase promoter. After second-strand synthesis, the reaction mixture was extracted with phenol–chloroform–isoamyl alcohol, and ds-cDNA was recovered by ethanol precipitation. *In vitro* transcription was performed by using a RNA transcription labeling kit (Enzo) with 10 μl of ds-cDNA template in the presence of a mixture of unlabeled ATP, CTP, GTP and UTP and biotin-labeled CTP and UTP [bio-11-CTP and bio-16-UTP (Enzo Life Sciences, Farmingdale, NY, USA)]. Biotin-labeled cRNA was purified by using an RNeasy affinity column (Qiagen, Valencia, CA, USA), and fragmented randomly to sizes ranging from 35 to 200 bases by incubating at 94°C for 35 min. The hybridization solutions contained 100 mM MES, 1 M NaCl, 20 mM EDTA and 0.01% Tween-20. The final concentration of fragmented cRNA was 0.05 μg/μl in the hybridization solution. After hybridization, the solutions were removed and GeneChips were washed and stained with streptavidin–phycoerythrin. GeneChips were read at a resolution of 6 μm with a Hewlett-Packard GeneArray Scanner. Initial data preparation (i.e. generation of CHP files) were performed by Affymetrix MICROARRAY SUITE v5.0. Normalization (quantile method) and calculation of signal intensities were performed with the software package RMA from the R project (http://www.r-project.org/). Data were based on four Affymetrix MGU74Av2 GeneChips (biological replicates) for each time-point per genotype (i.e. total of eight GeneChips per timepoint). Of the total 24 GeneChips, only one had to be repeated due to a negative quality report based on raw image and MAS5 analysis. Ratios of average signal intensity ($\log_2$) were then calculated for the probesets ($Nrl^{-/-}$ relative to wild-type) and then converted to an AFC. Statistical validation was performed on probesets showing a minimum AFC of 1.5. If due to low signal, any of these probesets were reported as having an absent signal (based on MAS5) in all GeneChips (i.e. for both genotypes) for a given time-point then it was reported as absent and reported signal values and relative expressions were ignored.

### FDR and *P*-values

The statistical method used to assign *P*-values to the fold-changes of gene responses is a two-step procedure based on the Benjamini and Yekutieli construction of FDRCI (63–65) on the fold-changes between the $Nrl^{-/-}$ and the wild-type response profiles (55). FDRCIs are $(1 - q)$% confidence intervals where the level '$q$' is corrected for error amplification inherent to performing multiple comparisons on many genes and many time-points. For specified minimum fold-change (fcmin) and a given level of significance $q$, a gene response is declared as 'positive' if the range of the FDRCI is either greater than fcmin (positive fold-change) or less than −fcmin (negative fold-change). The FDRCI *P*-value for a given gene is defined as the minimum level $q$ for which the gene's FDRCI does not intersect the interval [−fcmin, fcmin]. For this data, we formed a ranked list of genes according to increasing FDRCI significance level having minfc of 1.5 (0.58 $\log_2$). All probesets with a *P*-value $<1$ were reported.

### Q-PCR

RNA was treated with RQ1 DNAse (Promega, Madison, WI, USA) following manufacturer's guidelines. Oligo-dT-primed reverse transcription was performed using 2.5 μg of DNAse-treated total retinal RNA with Superscript II (Invitrogen). Primers for the validated genes were designed typically from the 3′ UTR region using Primer 3 (http://www-genome.wi.mit.edu/cgi-bin/primer/primer3). The PCR reactions on the cDNA template were then performed in triplicate in an I-cycler thermocycler with optical module (BioRad, Hercules, CA, USA). Amplified products were quantified based on the level of fluorescence of SybrGreen I (Molecular Probes, Eugene, OR, USA) in each reaction. Specificity of reactions was confirmed by melt curve analysis and gel electrophoresis. AFCs were then calculated based on the difference in the threshold cycles ($C_t$) between the $Nrl^{-/-}$ and the wild-type samples after normalization to *Hprt*.

### Clustering analysis

Clustering based on similarity of temporal expression profiles and visualization was performed using the software program Spotfire DecisionSite 7.2 (www.spotfire.com). The signal data of statistically significant differentially expressed genes were standardized to z-scores (66), and hierarchical clustering performed using the 'Euclidean distance' method.

### Annotation

Functional annotation of proteins was assigned through Gene Ontology (http://www.geneontology.org) or Locuslink (http://www.ncbi.nlm.nih.gov/LocusLink) classifications obtained through appropriate public databases such as NetAffx (http://www.netaffx.com/indexp2.jsp) (67) and DAVID (http://apps1.niaid.nih.gov/david/upload.asp) (68).

### ChIP analysis

Retinas were obtained from the C57BL/6 wild-type mice and snap frozen on dry ice. ChIP was performed using a commercial assay kit (Upstate Biotechnologies, Charlottesville, VA, USA). Briefly, four retinas were crosslinked in PBS containing proteinase inhibitors and a final concentration of 1% formaldehyde for 15 min at 37°C. The retinas were washed four times in ice-cold PBS with proteinase inhibitors and then incubated on ice for 15 min. The tissue was then sonicated on ice with 10 pulses of 20 sec. The remaining steps were performed as described by the manufacturer, using an anti-NRL polyclonal antibody (8).

The putative promoter region for each of the genes analyzed was determined using *in silico* methods (http://www.ncbi.nlm.nih.gov/mapview). Each promoter DNA sequence was analyzed using Matinspector (http://www.genomatix.de/index.html) and PCR primers were designed to flank putative AP1-like sites either predicted by Matinspector or predicted manually. If there was more than one AP-1 like site, the sequence element closest to the 5′ untranslated sequence was used. Equal amounts of input DNA, with and without antibody, were used in each PCR reaction.

## SUPPLEMENTARY MATERIAL

Supplementary Material is available at HMG Online.

## ACKNOWLEDGEMENTS

The authors thank S. Zareparsi, M.I. Othman and S.P. MacNee for discussions, and Sharyn Ferrara for administrative assistance. This research was supported by grants from the National Institutes of Health (EY11115 including administrative supplements, EY07003), The Foundation Fighting Blindness (Owings Mills, MD, USA) and Research to Prevent Blindness (RPB; New York, NY, USA). A.J.M is a recipient of a Tier 2 Canada Research Chair. J.S.F. is a recipient of an FFB-Canada post-doctoral fellowship. A.S. is Harold F. Falls Collegiate Professor and RPB Senior Scientific Investigator.

## REFERENCES

1. Masland, R.H. (2001) The fundamental plan of the retina. *Nat. Neurosci.*, **4**, 877–886.
2. Curcio, C.A., Sloan, K.R., Kalina, R.E. and Hendrickson, A.E. (1990) Human photoreceptor topography. *J. Comp. Neurol.*, **292**, 497–523.
3. Williams, D.S. (2002) Transport to the photoreceptor outer segment by myosin VIIa and kinesin II. *Vision Res.*, **42**, 455–462.
4. Tan, E., Wang, Q., Quiambao, A.B., Xu, X., Qtaishat, N.M., Peachey, N.S., Lem, J., Fliesler, S.J., Pepperberg, D.R., Naash, M.I. *et al.* (2001) The relationship between opsin overexpression and photoreceptor degeneration. *Invest. Ophthalmol. Vis. Sci.*, **42**, 589–600.
5. Pacione, L.R., Szego, M.J., Ikeda, S., Nishina, P.M. and McInnes, R.R. (2003) Progress toward understanding the genetic and biochemical mechanisms of inherited photoreceptor degenerations. *Annu. Rev. Neurosci.*, **26**, 657–700.
6. Rattner, A., Sun, H. and Nathans, J. (1999) Molecular genetics of human retinal disease. *Annu. Rev. Genet.*, **33**, 89–131.
7. Swaroop, A., Xu, J.Z., Pawar, H., Jackson, A., Skolnick, C. and Agarwal, N. (1992) A conserved retina-specific gene encodes a basic motif/leucine zipper domain. *Proc. Natl Acad. Sci. USA*, **89**, 266–270.
8. Swain, P.K., Hicks, D., Mears, A.J., Apel, I.J., Smith, J.E., John, S.K., Hendrickson, A., Milam, A.H. and Swaroop, A. (2001) Multiple phosphorylated isoforms of NRL are expressed in rod photoreceptors. *J. Biol. Chem.*, **276**, 36824–36830.
9. Mitton, K.P., Swain, P.K., Chen, S., Xu, S., Zack, D.J. and Swaroop, A. (2000) The leucine zipper of NRL interacts with the CRX homeodomain. A possible mechanism of transcriptional synergy in rhodopsin regulation. *J. Biol. Chem.*, **275**, 29794–29799.
10. Rehemtulla, A., Warwar, R., Kumar, R., Ji, X., Zack, D.J. and Swaroop, A. (1996) The basic motif-leucine zipper transcription factor Nrl can positively regulate rhodopsin gene expression. *Proc. Natl Acad. Sci. USA*, **93**, 191–195.
11. Pittler, S.J., Zhang, Y., Chen, S., Mears, A.J., Zack, D.J., Ren, Z., Swain, P.K., Yao, S., Swaroop, A. and White, J.B. (2004) Functional analysis of the rod photoreceptor cGMP phosphodiesterase alpha subunit gene promoter: Nrl and Crx are required for full transcriptional activity. *J. Biol. Chem.*, **279**, 19800–19807.
12. Lerner, L.E., Gribanova, Y.E., Ji, M., Knox, B.E. and Farber, D.B. (2001) Nrl and Sp nuclear proteins mediate transcription of rod-specific cGMP-phosphodiesterase beta-subunit gene: involvement of multiple response elements. *J. Biol. Chem.*, **276**, 34999–35007.
13. Bessant, D.A., Payne, A.M., Mitton, K.P., Wang, Q.L., Swain, P.K., Plant, C., Bird, A.C., Zack, D.J., Swaroop, A. and Bhattacharya, S.S. (1999) A mutation in NRL is associated with autosomal dominant retinitis pigmentosa. *Nat. Genet.*, **21**, 355–356.
14. Bessant, D.A., Payne, A.M., Plant, C., Bird, A.C., Swaroop, A. and Bhattacharya, S.S. (2000) NRL S50T mutation and the importance of 'founder effects' in inherited retinal dystrophies. *Eur. J. Hum. Genet.*, **8**, 783–787.
15. DeAngelis, M.M., Grimsby, J.L., Sandberg, M.A., Berson, E.L. and Dryja, T.P. (2002) Novel mutations in the NRL gene and associated clinical findings in patients with dominant retinitis pigmentosa. *Arch. Ophthalmol.*, **120**, 369–375.
16. Martinez-Gimeno, M., Maseras, M., Baiget, M., Beneito, M., Antinolo, G., Ayuso, C. and Carballo, M. (2001) Mutations P51U and G122E in retinal transcription factor NRL associated with autosomal dominant and sporadic retinitis pigmentosa. *Hum. Mutat.*, **17**, 520.
17. Bessant, D.A., Holder, G.E., Fitzke, F.W., Payne, A.M., Bhattacharya, S.S. and Bird, A.C. (2003) Phenotype of retinitis pigmentosa associated with the Ser50Thr mutation in the NRL gene. *Arch. Ophthalmol.*, **121**, 793–802.
18. Mears, A.J., Kondo, M., Swain, P.K., Takada, Y., Bush, R.A., Saunders, T.L., Sieving, P.A. and Swaroop, A. (2001) Nrl is required for rod photoreceptor development. *Nat. Genet.*, **29**, 447–452.
19. Akhmedov, N.B., Piriev, N.I., Chang, B., Rapoport, A.L., Hawes, N.L., Nishina, P.M., Nusinowitz, S., Heckenlively, J.R., Roderick, T.H., Kozak, C.A. *et al.* (2000) A deletion in a photoreceptor-specific nuclear receptor mRNA causes retinal degeneration in the rd7 mouse. *Proc. Natl Acad. Sci. USA*, **97**, 5551–5556.
20. Haider, N.B., Naggert, J.K. and Nishina, P.M. (2001) Excess cone cell proliferation due to lack of a functional NR2E3 causes retinal dysplasia and degeneration in rd7/rd7 mice. *Hum. Mol. Genet.*, **10**, 1619–1626.

21. Haider, N.B., Jacobson, S.G., Cideciyan, A.V., Swiderski, R., Streb, L.M., Searby, C., Beck, G., Hockey, R., Hanna, D.B., Gorman, S. *et al.* (2000) Mutation of a nuclear receptor gene, *NR2E3*, causes enhanced S cone syndrome, a disorder of retinal cell fate. *Nat. Genet.*, **24**, 127–131.
22. Livesey, F.J. and Cepko, C.L. (2001) Vertebrate neural cell-fate determination: lessons from the retina. *Nat. Rev. Neurosci.*, **2**, 109–118.
23. Nishida, A., Furukawa, A., Koike, C., Tano, Y., Aizawa, S., Matsuo, I. and Furukawa, T. (2003) Otx2 homeobox gene controls retinal photoreceptor cell fate and pineal gland development. *Nat. Neurosci.*, **6**, 1255–1263.
24. Ng, L., Hurley, J.B., Dierks, B., Srinivas, M., Salto, C., Vennstrom, B., Reh, T.A. and Forrest, D. (2001) A thyroid hormone receptor that is required for the development of green cone photoreceptors. *Nat. Genet.*, **27**, 94–98.
25. Zhang, J., Gray, J., Wu, L., Leone, G., Rowan, S., Cepko, C.L., Zhu, X., Craft, C.M. and Dyer, M.A. (2004) Rb regulates proliferation and rod photoreceptor development in the mouse retina. *Nat. Genet.*, **36**, 351–360.
26. DeRyckere, D. and DeGregori, J. (2002) Identification and characterization of transcription factor target genes using gene-targeted mice. *Methods*, **26**, 57–75.
27. Livesey, F.J., Furukawa, T., Steffen, M.A., Church, G.M. and Cepko, C.L. (2000) Microarray analysis of the transcriptional network controlled by the photoreceptor homeobox gene *Crx*. *Curr. Biol.*, **10**, 301–310.
28. Mu, X., Zhao, S., Pershad, R., Hsieh, T.F., Scarpa, A., Wang, S.W., White, R.A., Beremand, P.D., Thomas, T.L., Gan, L. *et al.* (2001) Gene expression in the developing mouse retina by EST sequencing and microarray analysis. *Nucl. Acids Res.*, **29**, 4983–4993.
29. Irizarry, R.A., Bolstad, B.M., Collin, F., Cope, L.M., Hobbs, B. and Speed, T.P. (2003) Summaries of Affymetrix GeneChip probe level data. *Nucl. Acids Res.*, **31**, e15.
30. Young, R.W. (1985) Cell differentiation in the retina of the mouse. *Anat. Rec.*, **212**, 199–205.
31. Irizarry, R.A., Hobbs, B., Collin, F., Beazer-Barclay, Y.D., Antonellis, K.J., Scherf, U. and Speed, T.P. (2003) Exploration, normalization, and summaries of high density oligonucleotide array probe level data. *Biostatistics*, **4**, 249–264.
32. Barash, Y., Dehan, E., Krupsky, M., Franklin, W., Geraci, M., Friedman, N. and Kaminski, N. (2004) Comparative analysis of algorithms for signal quantitation from oligonucleotide microarrays. *Bioinformatics*, **20**, 839–846.
33. Xi, J., Farjo, R., Yoshida, S., Kern, T.S., Swaroop, A. and Andley, U.P. (2003) A comprehensive analysis of the expression of crystallins in mouse retina. *Mol. Vis.*, **9**, 410–419.
34. Kennan, A., Aherne, A., Palfi, A., Humphries, M., McKee, A., Stitt, A., Simpson, D.A., Demtroder, K., Orntoft, T., Ayuso, C. *et al.* (2002) Identification of an IMPDH1 mutation in autosomal dominant retinitis pigmentosa (RP10) revealed following comparative microarray analysis of transcripts derived from retinas of wild-type and Rho(−/−) mice. *Hum. Mol. Genet.*, **11**, 547–557.
35. Taylor, R.E., Shows, K.H., Zhao, Y. and Pittler, S.J. (2001) A PDE6A promoter fragment directs transcription predominantly in the photoreceptor. *Biochem. Biophys. Res. Commun.*, **282**, 543–547.
36. Payne, A.M., Downes, S.M., Bessant, D.A., Taylor, R., Holder, G.E., Warren, M.J., Bird, A.C. and Bhattacharya, S.S. (1998) A mutation in guanylate cyclase activator 1A (GUCA1A) in an autosomal dominant cone dystrophy pedigree mapping to a new locus on chromosome 6p21.1. *Hum. Mol. Genet.*, **7**, 273–277.
37. Downes, S.M., Holder, G.E., Fitzke, F.W., Payne, A.M., Warren, M.J., Bhattacharya, S.S. and Bird, A.C. (2001) Autosomal dominant cone and cone–rod dystrophy with mutations in the guanylate cyclase activator 1A gene-encoding guanylate cyclase activating protein-1. *Arch. Ophthalmol.*, **119**, 96–105.
38. Naya, F.S. and Olson, E. (1999) MEF2: a transcriptional target for signaling pathways controlling skeletal muscle growth and differentiation. *Curr. Opin. Cell Biol.*, **11**, 683–688.
39. Parker, M.H., Seale, P. and Rudnicki, M.A. (2003) Looking back to the embryo: defining transcriptional networks in adult myogenesis. *Nat. Rev. Genet.*, **4**, 497–507.
40. Mori, M., Ghyselinck, N.B., Chambon, P. and Mark, M. (2001) Systematic immunolocalization of retinoid receptors in developing and adult mouse eyes. *Invest. Ophthalmol. Vis. Sci.*, **42**, 1312–1318.
41. Li, A., Zhu, X., Brown, B. and Craft, C.M. (2003) Gene expression networks underlying retinoic acid-induced differentiation of human retinoblastoma cells. *Invest. Ophthalmol. Vis. Sci.*, **44**, 996–1007.
42. Mollereau, B., Dominguez, M., Webel, R., Colley, N.J., Keung, B., de Celis, J.F. and Desplan, C. (2001) Two-step process for photoreceptor formation in *Drosophila*. *Nature*, **412**, 911–913.
43. Leong, M.L., Maiyar, A.C., Kim, B., O'Keeffe, B.A. and Firestone, G.L. (2003) Expression of the serum- and glucocorticoid-inducible protein kinase, Sgk, is a cell survival response to multiple types of environmental stress stimuli in mammary epithelial cells. *J. Biol. Chem.*, **278**, 5871–5882.
44. Heyninck, K., De Valck, D., Vanden Berghe, W., Van Criekinge, W., Contreras, R., Fiers, W., Haegeman, G. and Beyaert, R. (1999) The zinc finger protein A20 inhibits TNF-induced NF-kappaB-dependent gene expression by interfering with an RIP- or TRAF2-mediated transactivation signal and directly binds to a novel NF-kappaB-inhibiting protein ABIN. *J. Cell Biol.*, **145**, 1471–1482.
45. Wu, T., Chiang, S.K., Chau, F.Y. and Tso, M.O. (2003) Light-induced photoreceptor degeneration may involve the NF kappa B/caspase-1 pathway *in vivo*. *Brain Res.*, **967**, 19–26.
46. Jastrzebska, B., Filipek, A., Nowicka, D., Kaczmarek, L. and Kuznicki, J. (2000) Calcyclin (S100A6) binding protein (CacyBP) is highly expressed in brain neurons. *J. Histochem. Cytochem.*, **48**, 1195–1202.
47. Joo, J.H., Kim, J.W., Lee, Y., Yoon, S.Y., Kim, J.H., Paik, S.G. and Choe, I.S. (2003) Involvement of NF-kappaB in the regulation of S100A6 gene expression in human hepatoblastoma cell line HepG2. *Biochem. Biophys. Res. Commun.*, **307**, 274–280.
48. Claudepierre, T., Dalloz, C., Mornet, D., Matsumura, K., Sahel, J. and Rendon, A. (2000) Characterization of the intermolecular associations of the dystrophin-associated glycoprotein complex in retinal Muller glial cells. *J. Cell Sci.*, **113**, 3409–3417.
49. Claudepierre, T., Rodius, F., Frasson, M., Fontaine, V., Picaud, S., Dreyfus, H., Mornet, D. and Rendon, A. (1999) Differential distribution of dystrophins in rat retina. *Invest. Ophthalmol. Vis. Sci.*, **40**, 1520–1529.
50. Ribelayga, C., Wang, Y. and Mangel, S.C. (2004) A circadian clock in the fish retina regulates dopamine release via activation of melatonin receptors. *J. Physiol.*, **554**, 467–482.
51. Tosini, G. and Fukuhara, C. (2003) Photic and circadian regulation of retinal melatonin in mammals. *J. Neuroendocrinol.*, **15**, 364–369.
52. Dorrell, M.I., Aguilar, E., Weber, C. and Friedlander, M. (2004) Global gene expression analysis of the developing post natal mouse retina. *Invest. Ophthalmol. Vis. Sci.*, **45**, 1009–1019.
53. Kremerskothen, J., Plaas, C., Buther, K., Finger, I., Veltel, S., Matanis, T., Liedtke, T. and Barnekow, A. (2003) Characterization of KIBRA, a novel WW domain-containing protein. *Biochem. Biophys. Res. Commun.*, **300**, 862–867.
54. Zareparsi, S., Hero, A.O., Zack, D.J., Williams, R.W. and Swaroop, A. (2004) Seeing the unseen: Microarray-based gene expression profiling in vision. *Invest. Ophthalmol. Vis. Sci.*, in press.
55. Hero, A.O., Fleury, G., Mears, A.J. and Swaroop, A. (2004) Multicriteria gene screening for analysis of differential expression with DNA microarrays. *EURASIP JASP*, **2004**, 43–52.
56. Hoang, Q.V., Linsenmeier, R.A., Chung, C.K. and Curcio, C.A. (2002) Photoreceptor inner segments in monkey and human retina: mitochondrial density, optics, and regional variation. *Vis. Neurosci.*, **19**, 395–407.
57. Perkins, G.A., Ellisman, M.H. and Fox, D.A. (2003) Three-dimensional analysis of mouse rod and cone mitochondrial cristae architecture: bioenergetic and functional implications. *Mol. Vis.*, **9**, 60–73.
58. Farjo, R., Yu, J., Othman, M.I., Yoshida, S., Sheth, S., Glaser, T., Baehr, W. and Swaroop, A. (2002) Mouse eye gene microarrays for investigating ocular development and disease. *Vision Res.*, **42**, 463–470.
59. Chowers, I., Gunatilaka, T.L., Farkas, R.H., Qian, J., Hackam, A.S., Duh, E., Kageyama, M., Wang, C., Vora, A., Campochiaro, P.A. *et al.* (2003) Identification of novel genes preferentially expressed in the retina using a custom human retina cDNA microarray. *Invest. Ophthalmol. Vis. Sci.*, **44**, 3732–3741.
60. Mu, X., Beremand, P.D., Zhao, S., Pershad, R., Sun, H., Scarpa, A., Liang, S., Thomas, T.L. and Klein, W.H. (2004) Discrete gene sets depend on POU domain transcription factor Brn3b/Brn-3.2/POU4f2 for their

expression in the mouse embryonic retina. *Development*, **131**, 1197–1210.
61. Jones, B.W., Watt, C.B., Frederick, J.M., Baehr, W., Chen, C.K., Levine, E.M., Milam, A.H., Lavail, M.M. and Marc, R.E. (2003) Retinal remodeling triggered by photoreceptor degenerations. *J. Comp. Neurol.*, **464**, 1–16.
62. Marc, R.E., Jones, B.W., Watt, C.B. and Strettoi, E. (2003) Neural remodeling in retinal degeneration. *Prog. Retin. Eye Res.*, **22**, 607–655.
63. Reiner, A., Yekutieli, D. and Benjamini, Y. (2003) Identifying differentially expressed genes using false discovery rate controlling procedures. *Bioinformatics*, **19**, 368–375.
64. Benjamini, Y., Drai, D., Elmer, G., Kafkafi, N. and Golani, I. (2001) Controlling the false discovery rate in behavior genetics research. *Behav. Brain Res.*, **125**, 279–284.
65. Benjamini, Y. and Hochberg, Y. (1995) Controlling the false discovery rate: a practical and powerful approach to multiple testing. *J. R. Stat. Soc.*, **57**, 289–300.
66. Matoba, R., Kato, K., Kurooka, C., Maruyama, C., Sakakibara, Y. and Matsubara, K. (2000) Correlation between gene functions and developmental expression patterns in the mouse cerebellum. *Eur. J. Neurosci.*, **12**, 1357–1371.
67. Liu, G., Loraine, A.E., Shigeta, R., Cline, M., Cheng, J., Valmeekam, V., Sun, S., Kulp, D. and Siani-Rose, M.A. (2003) NetAffx: Affymetrix probesets and annotations. *Nucl. Acids Res.*, **31**, 82–86.
68. Dennis, G., Jr, Sherman, B.T., Hosack, D.A., Yang, J., Gao, W., Lane, H.C. and Lempicki, R.A. (2003) DAVID: database for annotation, visualization, and integrated discovery. *Genome Biol.*, **4**, P3.

# 7. RDH5遺伝子に異常を有する白点状眼底における錐体と杆体の変性

近藤峰生、丹羽泰洋、上野真治、中村誠、寺崎浩子、三宅養三
(名古屋大)

本研究では、白点状眼底 (fundus albipunctatus) における錐体機能異常の頻度とその原因部位、および杆体変性の合併について調査した。過去10年間に当科を受診した白点状眼底患者でRDH5遺伝子に異常が確認された16例を対象とし、正常者48例の結果と比較した。白点状眼底の約38%に広範囲な錐体ERGの低下がみられた。ERGの成分解析により、白点状眼底において錐体ERGの振幅が低下している理由は、錐体視細胞そのものの変性 (外節の短縮あるいは視細胞数減少) によるものであることがわかった。また、錐体変性を伴う症例では、杆体の変性も合併しやすいことがわかった。

## A. 研究目的

白点状眼底の中には、錐体系網膜電図 (ERG) に異常を示すものが存在することが知られている (Miyake et al. 1992; Nakamura et al. 2000)。今回我々は、最近10年間に当科を受診した白点状眼底における錐体機能異常の頻度とその原因部位を調べた。また、このような症例における杆体変性の合併についても調べた。

## B. 研究方法

過去10年間に当科を受診した連続的な白点状眼底で、RDH5遺伝子に異常が確認された16例 (平均25.4歳) を対象とし、正常者50例の結果と比較した。標準的な錐体ERGのb波の振幅と潜時を計測した。また、強力な刺激光を用いて錐体a波を記録し、Hoodらのfitting方法により視細胞電位の*Rm* (最大振幅値) と*S* (感度) を算出した。また、3時間の十分な暗順応後に杆体ERGを記録した。

## (倫理面への配慮)

全ての対象患者に検査の目的と方法を十分に説明し、informed consentを得た。

## C. 研究結果

(1) 白点状眼底の16例中、錐体ERGの振幅が正常群の下限値よりも小さいものは6例であった (図1)。 (2) 患者で錐体ERGの振幅が小さい症例では、a波のfitting解析の結果では*Rm* (最大振幅) が正常値より明らかに低下していた。(3)患者で錐体ERGが低下している群では杆体ERGの振幅も低下している傾向がみられた。

## D. 考察

今回の結果から、白点状眼底患者の一部 (約38%) は錐体-杆体変性を合併することがわかった。さらに変性の重症度と年齢の関係の解析により、錐体および杆体の変性は加齢に伴い進行することが推測された。

図1

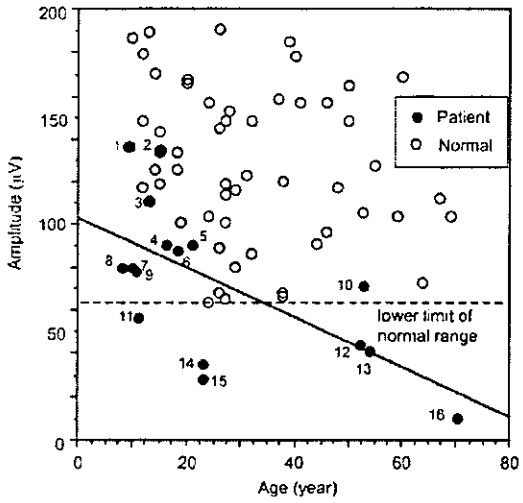


## E．結論

(1) 白点状眼底では、約 38%に錐体 ERG の低下がみられ、その異常は加齢により進行する。(2) 白点状眼底で錐体 ERG の振幅が小さい理由は、錐体視細胞そのものの変性（外節の短縮あるいは視細胞数減少）によるものである。(3) 錐体変性を伴う白点状眼底では、杆体の変性も合併しやすい。

## F．健康危険情報

なし

## G．研究発表

### 1．論文発表

1. Kondo M et al: Peripheral cone dystrophy: A variant of cone dystrophy with predominant dysfunction in the peripheral cone system. Ophthalmology 111, 732-739, 2004.

2.Ueno S et al: Luminance dependence of neural components that underlies the primate photopic Electroretinogram. Invest Ophthalmol Vis Sci 45, 1033-1040, 2004

3. Khan NW et al: Primate retinal signaling pathways: suppressing ON-pathway activity in monkey with glutamate analogues mimics human CSNB1-NYX genetic night blindness. J Neurophysiol 93,481-492, 2005

4. Niwa Y et al: Cone and rod dysfunction in fundus albipunctatus with RDH5 mutation: Electrophysiological study. Invest Ophthalmol Vis Sci. in press.

### 2．学会発表

1.Kondo M: Use of ERG to understand the pathophysiology of congenital stationary night blindness. Symposium in Annual Meeting of the Association for Research in Vision and Ophthalmology (ARV0). Fort Laudadale, Florida, 2004

2.Kondo M: Multifocal pupillary response field in normal subjects and patients with visual field defects. Symposuim in XVI International Congress of Eye Research. Sydney, 2004

## H．知的財産権の出願・登録状況

### 1．特許取得

なし

### 2．実用新案登録

なし

### 3．その他

なし

## I．参考文献

1.Miyake Y et al: Fundus albipunctatus

associated with cone dystrophy. Br J Ophthalmol 76:375-379, 1992
2. Nakamura M et al: A high association with cone dystrophy in Fundus albipunctatus caused by mutations of the RDH5 gene. Invest Ophthalmol Vis Sci 41, 3925-3932, 2000

# 8. クリスタリン網膜症患者のCYP4V2遺伝子変異検索

板橋俊隆、和田裕子、川村后幸、多田麻子、佐藤　肇、遠藤麻衣、玉井　信
（東北大）

**研究要旨**　クリスタリン網膜症は、網膜・角膜に結晶沈着、脈絡膜毛細管板の萎縮を認める疾患であり、2004年にCYP4V2遺伝子がその原因遺伝子であると報告された。今回我々は、日本人クリスタリン網膜症患者におけるCYP4V2遺伝子異常解析の結果と臨床像について報告する。眼科的検索にてクリスタリン網膜症と診断した女性6例、男性1例を対象とし、CYP4V2遺伝子を用いてPCR－Direct sequence法にて遺伝子変異解析を施行した。変異を確認した症例については眼科的検索を行い、臨床像を詳細に検討した。7例中5例に既報告のIVS6-8delTCATACAGGTCATCGCG/insGCをホモ接合体で認め、1例に新規変異Trp340Stop変異をホモ接合体で認めた。変異を認めた患者には、網膜に閃輝性の結晶沈着物を認めたが、進行した症例では脈絡膜萎縮が強く、結晶沈着物は僅かであった。日本人クリスタリン網膜症はCYP4V2遺伝子異常が原因になる事を確認し、IVS6-8delTCATACAGGTCATCGCG/insGC変異は日本人患者の高頻度変異であると考えられた。

## A．研究目的

クリスタリン網膜症は、1937年、Biettiらにより網膜・角膜輪部表層に結晶沈着、網膜色素上皮・脈絡膜毛細管板の萎縮を認める常染色体劣性遺伝を示す症例が報告された[1]。その後、角膜に結晶沈着を認めない例が多数報告され、常染色体劣性遺伝を示さない例も報告された[2]。その後2004年、Liらにより CYP4V2 遺伝子がクリスタリン網膜症の原因遺伝子であると報告された[3]。我々は、日本人クリスタリン網膜症患者に対して CYP4V2 遺伝子を用いた変異検索と、臨床像を含めた検討を行う事を目的とした。

## B．研究方法

眼科的検索によりクリスタリン網膜症と診断した女性6例、男性1例を対象とした。遺伝子解析にインフォームド・コンセントを得た後、患者の抹消血白血球よりゲノムDNAを抽出した。CYP4V2遺伝子のエクソン1～11の全翻訳領域を覆うようにプライマーの設定を行い、Polymerase chain reaction (PCR)にて増幅した。その後Direct sequence法にて塩基配列の決定を行い解析した。眼科的検索は、矯正視力、ゴールドマン動的量的視野、網膜電位図（ERG)、眼底検査、蛍光眼底撮影、スペキュラーマイクロスコープを施行した。

## C．研究結果

遺伝子変異解析の結果、5家系6例にIVS6-8delTCATACAGGTCATCGCG/insGC変異を確認し、1家系1例に新規Trp340Stop変異を確認した。

変異を確認した患者の臨床像は、初発症状として夜盲を呈したのが3例で、全ての症

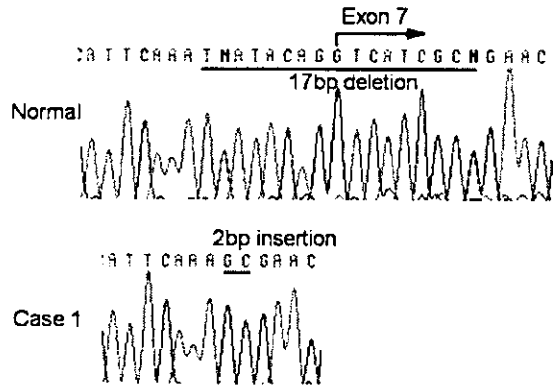


**図 1　シークエンス**
**IVS6-8delTCATACAGGTCATCGCG/insGC 変異**

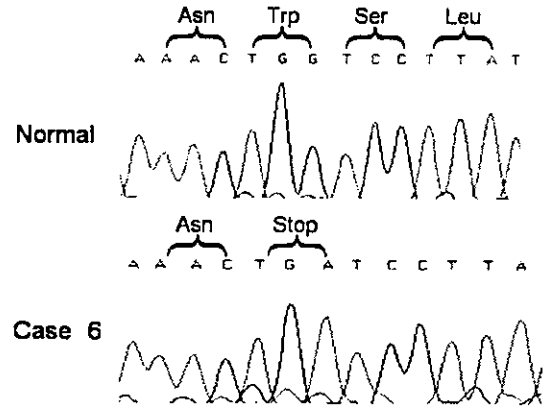


**図 2　シークエンス　Trp340Stop 変異**

例で 40 歳台での発症であった。視力は(0.02)から(1.5)と様々であった。ゴールドマン視野は 3 例に傍中心暗点を認め、2 例で求心性狭窄を示し、1 例は島状の視野を呈した。網膜電位図では、1 例は Scotopic、Standard flash、Photopic、30Hz flicker の全ての ERG が正常であったが、2 例では全ての ERG で消失型であった。眼底所見は、軽症なものでは網膜が粗雑で閃輝性白斑を確認できたが、重症なものでは脈絡膜毛細管板の萎縮を来たし、結晶沈着を確認できなかった。蛍光眼底造影所見では、網膜色素上皮の萎縮により過蛍光を示すものと、脈絡膜毛細管板の萎縮を来たして低蛍光を示すものがあった。Case 1、2、3 ではスペキュラーマイクロスコープにて角膜の結晶沈着物を確認した[4]。

## D．考察

IVS6-8delTCATACAGGTCATCGCG/insGC 変異は、日本人クリスタリン網膜症における高頻度変異と考えられた。変異を認めた患者の臨床像について検討したが、視力、視野、眼底所見、網膜電位図のいずれにおいても軽症なものから重症なものまで様々であり、表現型の多様性を認めた。今回変異を確認した 6 症例では、50 才台で急速に進行する傾向が認められた。

## E．結論

日本人クリスタリン網膜症 6 家系 7 例に CYP4V2 遺伝子変異を認め、そのうち IVS6-8delTCATACAGGTCATCGCG/insGC 変異は、日本人クリスタリン網膜症の高頻度変異であることが示唆された。表現型の多様性を認めたが、我々の 6 家系では 40 代で発症し、50 代より急速な視機能低下を示した[5]。

## F．健康危険情報

なし

## G．研究発表

### 1．論文発表

1. Itabashi T, Wada Y, Kawamura M, Sato H, Tamai M. Clinical features of Japanese families with a 402delT or a 555-556delAG mutation in choroideremia gene. Retina.24: 940-945, 2004

2. Itabashi T, Wada Y, Sato H, Kawamura M, Shiono T, Tamai M. Novel 615delC mutation in the CRX gene in a Japanese family with cone-rod dystrophy. Am J Ophthalmol. 138: 876-877, 2004.

**２．学会発表**

1. 板橋俊隆　他　「*CRX*, *Peripherin//RDS*、*GUCY2D*遺伝子を用いた遺伝子変異解析」　第108回日本眼科学会（2004年4月）
2. 板橋俊隆　他　「CRX遺伝子新規615delC変異を認めた錐体桿体ジストロフィの１例」　第58回日本臨床眼科学会（2004年11月）
3. Itabashi T, Wada Y, Sato H, Kawamura M, Tada A, Tamai M. Three Novel Mutations in The *RPGR* Gene Exon ORF15 in Three Japanese Families Associated with X-linked Retinitis Pigmentosa. 2004 ARVO, Florida
4. Itabashi T, Wada Y, Sato H, Kawamura M, Tada A, Tamai M. Five Novel Mutations in The *RPGR* Gene in Five Japanese Families Associated with X-linked Retinitis Pigmentosa. RD2004, Perth

**Ｈ．知的財産権の出願・登録状況**

**１．特許取得**

なし

**２．実用新案登録**

なし

**３．その他**

なし

**Ｉ．参考文献**

1. Bietti G. Ueber familiares Vorkmmen von Retinitis punctata albescence (Verbunden mit " Dystrophia marginalis cristallinea cornea ). Glitzen des Glaskopers und andeen degenerativen Augenveranderungen Klin Mbl Augenhelik. 99: 737-756, 1937.
2. Francois J, and de Laey J J. Bietti's crystalline fundus dystrophy. Ann Ophthalmol. 10: 709-716, 1978.
3. Li A, Jiao X, Munier EL at al. Bietti crystalline corneoretinal dystrophy is caused by mutations in the novel gene CYP4V2.Am J Hum Genet. 74: 817-826, 2004.
4. Wada Y, Abe T, Shiono T, Tamai M. Specular microscopic findings of corneal deposits in patients with Bietti's crystalline corneal retinal dystrophy. Br J Ophthalmol. 83: 1095, 1999.
5. Wada Y, et al. Screening for Mutations in *CYP4V2* Gene in Japanese Patients With Bietti's Crystalline Corneoretinal Dystrophy. *Am J Ophthalmol* (in press)

# CLINICAL FEATURES OF JAPANESE FAMILIES WITH A 402DELT OR A 555–556DELAG MUTATION IN CHOROIDEREMIA GENE

TOSHITAKA ITABASHI, MD, YUKO WADA, MD, MIYUKI KAWAMURA, MD, HAJIME SATO, MD, MAKOTO TAMAI, MD

**Purpose:** To characterize the clinical features of two Japanese families with choroideremia associated with a 402delT and a 555–556delAG mutation in the choroideremia gene (*CHM*).

**Methods:** Four affected members and one obligate carrier from two Japanese families with choroideremia were studied. To detect mutations of the *CHM* gene, the products of polymerase chain reaction were directly sequenced in both directions. The ophthalmologic examination included best-corrected visual acuity, slit-lamp examination, fundus examination, kinetic perimetry, electroretinography, and fluorescein angiography.

**Results:** A 402delT and a 555–556delAG mutation were found in two Japanese families with choroideremia. All affected members had night-blindness, progressive constriction of the visual field, chorioretinal atrophy, and mottled appearance of the retinal pigment epithelium. The obligate carrier had mild patchy areas of retinal pigment epithelial atrophy with no visual symptoms.

**Conclusion:** The authors found a 402delT and a 555–556delAG mutation in the *CHM* gene, one of which (402delT) is a novel mutation. They conclude that these mutations cause choroideremia in Japanese families.

**RETINA** 24:940–945, 2004

Choroideremia is an X-linked disorder characterized by night-blindness, constricted visual field, and a slow, progressive atrophy of the choroid, retina, and retinal pigment epithelium (RPE). The carriers of choroideremia have no symptoms of night-blindness and constricted visual field; however, they have characteristic fundus changes, such as peppery hyperpigmentation or patchy areas of chorioretinal atrophy. The candidate gene for choroideremia, designated *CHM*, was isolated by positional cloning,[1–3] and the complete human *CHM* gene was cloned in 1994.[4] The *CHM* gene is located on chromosome Xq21.2 and is expressed in the retina, choroid, RPE, and nonocular tissues.[5–7] It is made up of 653 amino acids and encodes the Rab escort protein (rep-1) that functions with Rab to regulate intracellular trafficking. To date, many mutations of the *CHM* gene have been reported in different ethnic populations.[1–16]

Because patients with choroideremia have mutations in the *CHM* gene, molecular genetic analysis of

From the Department of Ophthalmology, Tohoku University School of Medicine, Sendai, Japan.

This study was supported in part by a grant from the Research Committee on Chorioretinal Degenerations and Optic Atrophy, the Ministry of Health, Labor and Welfare of the Japanese government (T.I.), Tokyo, and a Grant-In-Aid for Scientific Research from the Ministry of Education, Science, and Culture of the Japanese government (Y.W., A-14704044), Tokyo, Japan.

Reprint requests: Toshitaka Itabashi, MD, Department of Ophthalmology, Tohoku University School of Medicine, 1–1 Seiryo-machi, Aoba-ku, Sendai 980–8574, Japan; e-mail: ita@oph.med.tohoku.ac.jp

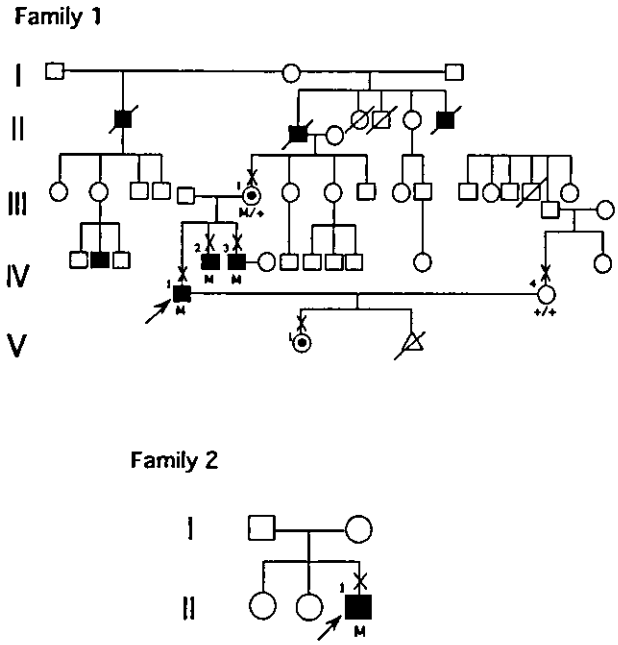


Fig. 1. Pedigrees of two Japanese families with choroideremia showing affected (solid symbols) and unaffected (open symbols) members. Squares, male members; circles, female members; X, individuals examined; dot in the circle, carrier; arrow, proband.

the *CHM* gene plays an important role in not only making a correct diagnosis but also genetic counseling.

The aim of this study was to assess the ocular findings in two Japanese families with choroideremia associated with two mutations in the *CHM* gene, one of which is a newly identified mutation.

## Materials and Methods

We examined four affected men and one carrier woman from two unrelated families (Figure 1). The ophthalmic examination included best-corrected visual acuity, slit-lamp biomicroscopy, kinetic perimetry, funduscopy, fluorescein angiography (FA), and electroretinography (ERG). The ERG recordings were performed under conditions that conformed to the International Society for Clinical Electrophysiology of Vision standards.[17] ERGs were elicited by a single flash or a 30-Hz flicker red light under light-adapted conditions for cone-isolated responses, a dim blue flash after 30 minutes of dark-adaptation for rod-isolated responses, and a standard white flash in dark-adapted conditions for the maximal mixed rod-cone response.

We analyzed the four affected members and one obligate carrier for mutations for the *CHM* gene. Genomic DNA was isolated from the leukocytes of each patient's blood using a protocol described in detail.[18] The genomic DNA was amplified from exon 1 to exon 15 of the *CHM* gene by polymerase chain

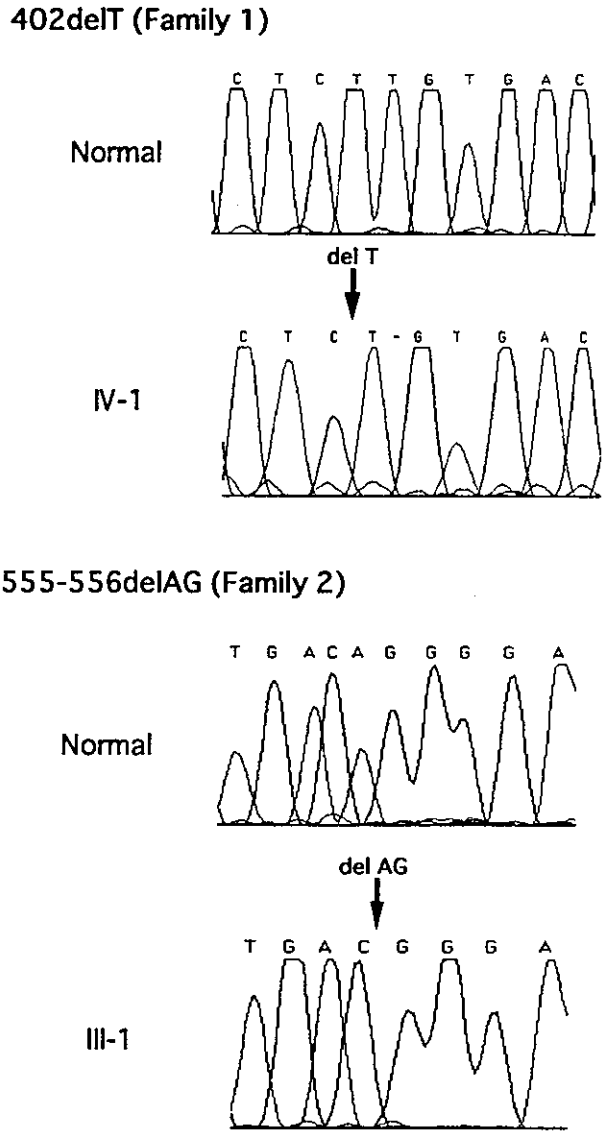


Fig. 2. Results of sequencing analysis. The upper sequence, normal allele; the bottom sequences, a mutant allele from Patient IV-1 of Family 1 with a 402delT mutation, and a mutant allele from Patient II-1 of Family 2 with a 555–556delAG mutation.

reaction (PCR). Fifteen sets of oligonucleotide primer pairs were used to amplify the entire coding region of the *CHM* gene. The PCR products were directly sequenced on an ABI3100 sequencer in both directions (Applied Biosystems, Perkin Elmer).

Informed consent was obtained from all patients before entry into this study.

## Results

### *DNA Analysis*

Two mutations were found in the *CHM* gene: a 402delT and a 555–556delAG mutation in exon 5 of

Table 1. Clinical Findings of Patients Associated with Mutation in the CHM Gene

| Patient | Family | Age, yr | Sex | Mutation | Age at onset of night blindness, yr | Age at onset of field loss, yr | Biomicroscopic findings | Fundus finding |
|---|---|---|---|---|---|---|---|---|
| IV-1 | 1 | 29 | M | 402delT | 12 | 29 | Normal | AN, CRA |
| | | | | | | | Normal | AN, CRA |
| IV-2 | 1 | 26 | M | 402delT | 21 | 21 | Normal | Mild CRA, mottled RPE |
| | | | | | | | Normal | Mild CRA, mottled RPE |
| IV-3 | 1 | 23 | M | 402delT | Not determined | Not determined | Normal | AN, mottled RPE |
| | | | | | | | Normal | AN, mottled RPE |
| III-1 | 1 | 54 | F | 402delT | Not determined | Not determined | Senile cataract | Peppery hyperpigmentation |
| | | | | | | | Senile cataract | Peppery hyperpigmentation |
| III-1 | 2 | 24 | M | 555–556delAG | 10 | 24 | Normal | CRA, mottled RPE |
| | | | | | | | Normal | CRA, mottled RPE |

AN = attenuation of retinal vessels; CRA = chorioretinal atrophy; RPE = retinal pigment epithelium.



Table 2. Visual Function in Patients With Mutation in the CHM Gene

| Patient | Family | Visual acuity | Manifest refraction | Fluorescein angiography | Electroretinogram | | | |
|---|---|---|---|---|---|---|---|---|
| | | | | | Scotopic b-wave | Bright flash b-wave | Photopic b-wave | 30 Hz flicker, μV |
| IV-1 | 1 | 1.0 OD | −0.75 −0.75 × 158 | Hypo F, Hyper F | Nonrecordable | Reduced to 14% of the normal mean | Reduced to 11% of the normal mean | 19.25 |
| | | 1.0 OS | 0.0 −1.00 × 175 | Hypo F, Hyper F | | | | 29.25 |
| IV-2 | 1 | 1.5 OD | +0.25 +0.5 × 63 | Hypo F, D Hyper F | Reduced to 5% of the normal mean | Reduced to 18% of the normal mean | Reduced to 34% of the normal mean | 59.25 |
| | | 1.5 OS | 0.0 −0.5 × 155 | Hypo F, D Hyper F | | | | 50.25 |
| IV-3 | 1 | 2.0 OD | +0.5 −0.5 × 149 | Granular Hypo F | Reduced to 22% of the normal mean | Reduced to 29% of the normal mean | Reduced to 34% of the normal mean within normal range | 57.75 |
| | | 2.0 OS | 0.0 −0.5 × 4 | Granular Hypo F | | | | 55.75 |
| III-1 | 1 | 1.0 OD | −1.5 | Hyper F | Within normal range | Within normal range | | 130.75 |
| | | 1.0 OS | −1.5 | Hyper F | | | | 101.25 |
| III-1 | 2 | 1.0 OD | +0.25 −2.75 × 3 | Granular Hyper F | Nonrecordable | Nonrecordable | Nonrecordable | Nonrecordable |
| | | 1.0 OS | +0.25 −2.0 × 180 | Granular Hyper F | | | | |

OD = right eye; Hypo F = hypofluorescence; Hyper F = hyperfluorescence; OS = left eye; D Hyper F = diffuse hyperfluorescence.
Normal mean amplitude of electroretinograms in our clinic: scotopic b-wave, 230.1 μV; bright flash b-wave, 560.2 μV; photopic b-wave, 110.3 μV; flicker b-wave, 127.5 μV.

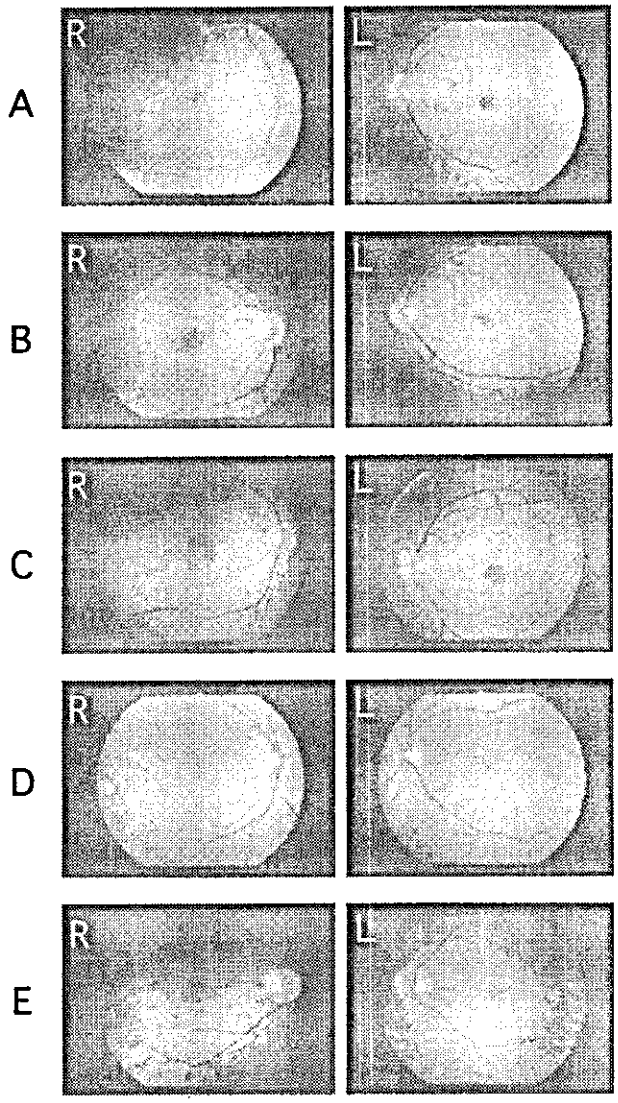


Fig. 3. Fundus photographs. **A,** Fundus photographs of Patient IV-1. Chorioretinal atrophy and attenuation of retinal vessels can be seen in both eyes. **B,** Fundus photographs of Patient IV-2 showing mild chorioretinal atrophy around the optic disk and mottled appearance of retinal pigment epithelium (RPE) in both eyes. **C,** Fundus photographs of Patient IV-3 showing mottled appearance of RPE in both eyes, and pigment clumping in the right eye. **D,** Fundus photographs of Patient III-1 showing patchy atrophic areas of RPE. **E,** Fundus photographs of Patient II-1 of Family 2 show chorioretinal atrophy with exposure of the choroidal vessels, pigmented stippling, and mottled appearance of RPE in both eyes.

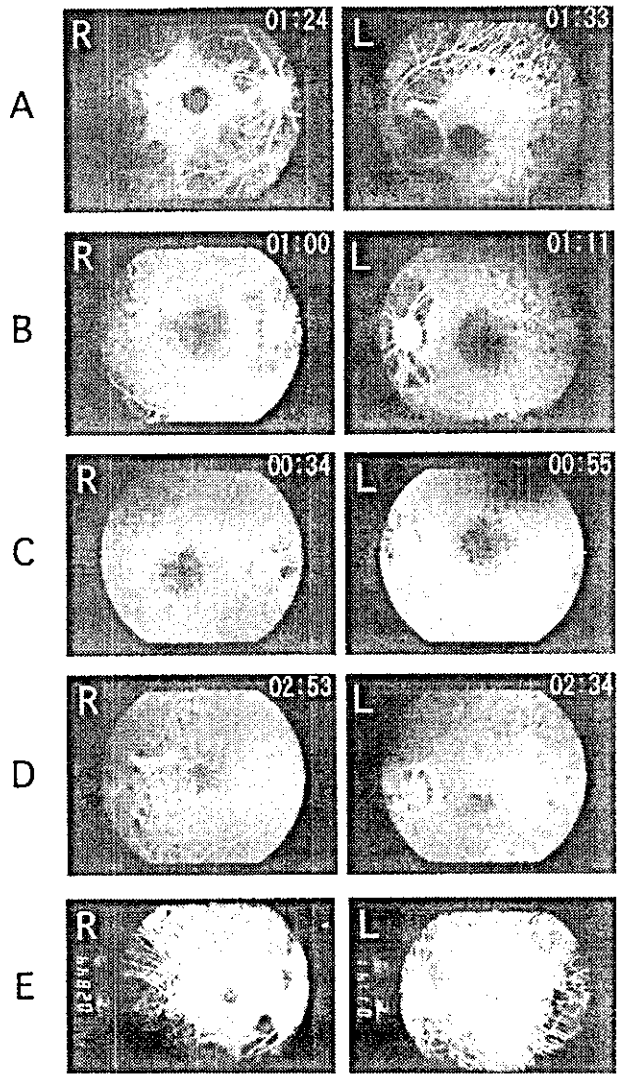


Fig. 4. Fluorescein angiography (FA). **A,** FA of Patient IV-1 of Family 1. The combination of hyperfluorescent and hypofluorescent areas is seen. **B,** FA of Patient IV-2 of Family 1 shows granular hyperfluorescence in the posterior pole and hypofluorescence around the optic disk. **C,** FA of Patient IV-3 of Family 1 shows granular hyperfluorescence in the posterior pole. **D,** FA of Patient III-1 showing granular hyperfluorescence around the macula in the right eye, and granular hyperfluorescence in the left posterior pole. **E,** FA of Patient II-1 of Family 2 showing granular hyperfluorescence corresponding to the atrophy of the retinal pigment and exposure of choroidal vessels.

the *CHM* gene (Figure 2). These mutations resulted in a frameshift and premature termination at codon 125 and 182, respectively. In Family 1, three affected men had a hemizygous 402delT mutation, and the obligate carrier was heterozygous for this mutation. In Family 2, one affected man had a hemizygous 555–556delAG mutation.

## Case Report

The four patients and one obligate carrier from two unrelated families associated with the 402delT and a 555–556delAG mutation in the *CHM* gene were examined and their clinical characteristics are summarized in Tables 1 and 2. In addition, Patient IV-1 of Family 1 requested genetic counseling for the planning of a second child.

The ages of the four patients ranged from 23 to 29 years. Three of the four affected patients had night-blindness from their early teens. The visual acuity of these patients ranged from 1.0 to 2.0, which indicated all patients had preserved central vision.

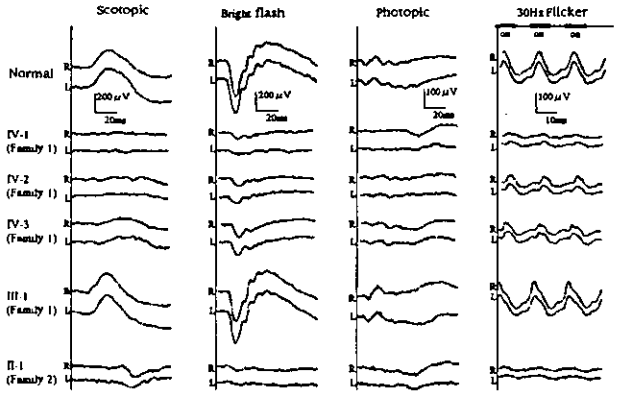


Fig. 5. Electroretinograms (ERGs) of four affected members and one carrier. The obligate carrier has normal amplitudes of all components of the ERGs. The ERGs of the affected members are mildly reduced to nonrecordable ERGs. These changes are correlated with the fundus changes. R, right eye; L, left eye. Patients are described in detail in Report of Cases.

Fundus examination of Patients IV-1 and IV-2 of Family 1 and II-1 of Family 2 disclosed chorioretinal atrophy with sparing of the macular region, exposure of the choroidal vessels, and mottled appearance of the RPE in both eyes. Patient IV-3 of Family 1, a 23-year-old man who was the youngest brother of Family 1, showed attenuation of the retinal vessels and mottled appearance of the RPE in both eyes. There was also pigment clumping in the right eye (Figure 3).

FA of Patients IV-1 and IV-2 of Family 1 and II-1 of Family 2 revealed a combination of hypofluorescence and hyperfluorescence with granular hyperfluorescence in the posterior poles, and the choroidal vessels were seen in bold relief against the hypofluorescent areas in the periphery of both eyes. Fluorescein angiography of IV-3 of Family 1 showed hyperfluorescent areas corresponding to the atrophy of the RPE in the posterior poles (Figure 4).

The scotopic b-waves were severely reduced in IV-2 and IV-3 of Family 1, and nonrecordable in IV-1 of Family 1. The scotopic, photopic, and 30 Hz flicker ERGs were severely reduced in all patients of Family 1. The scotopic, bright flash, photopic, and 30 Hz flicker ERGs were nonrecordable in Patient II-1 of Family 2 (Figure 5).

Kinetic visual field testing of IV-1 of Family 1 showed constricted visual field with I-2-e isopter and enlargement of the blind spot in the left eyes and constricted visual field with V-4-e and I-2-e isopters in the right eyes. Kinetic visual field testing of Patients IV-2 and IV-3 of Family 1 and II-1 of Family 2 showed ring scotomas and constricted visual fields with I-2e or I-4e isopters in both eyes (Figure 6).

Patient III-1 of Family 1, the 54-year-old mother of the three patients of Family 1, had no visual impairments. Her visual acuity was corrected to 1.0 in the right eye with −1.5 D sphere and 1.0 in the left eye with −1.5 D sphere. Slit-lamp biomicroscopic examination showed normal cornea, anterior chamber, iris, anterior vitreous, and senile cataracts in both eyes.

Fundus examination revealed peppery hyperpigmentation in both eyes (Figure 3). FA showed hyperfluorescent areas corresponding to the atrophy of the RPE in the posterior poles (Figure 4).

Her scotopic, bright flash, photopic, and 30 Hz flicker ERGs were normal (Figure 5) as were her kinetic visual fields (Figure 6).

We were not able to perform the molecular genetic analysis and ophthalmologic examination on the other members of Family 2, because consent was not obtained.

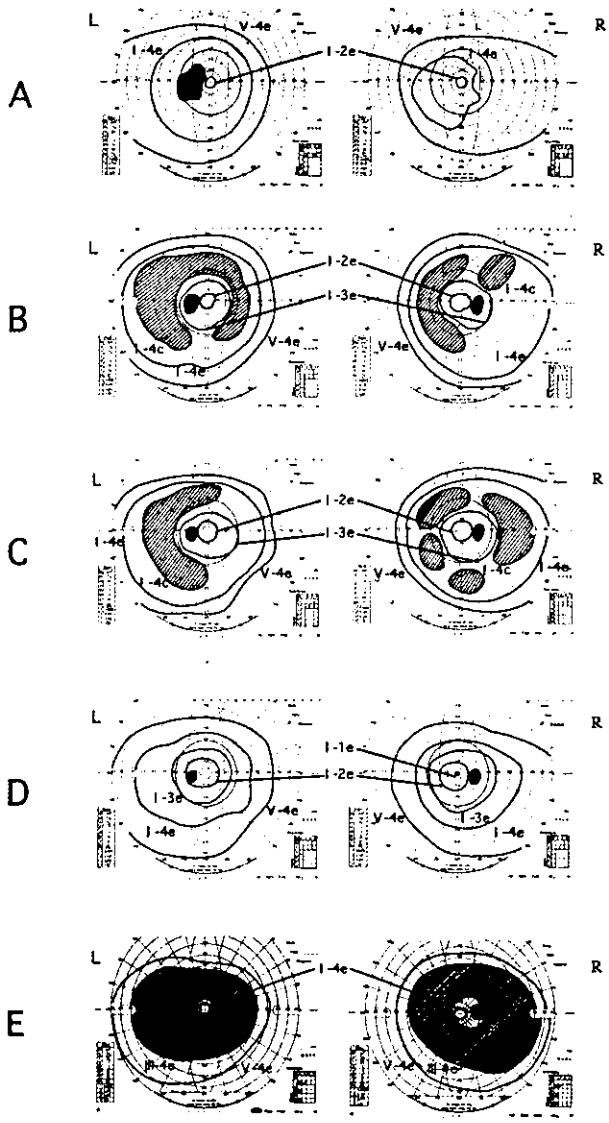


Fig. 6. Results of Goldmann visual fields of Patient IV-1 of Family 1. (A) Patient IV-2; (B) Patient IV-3; (C) Patient III-1; and (D) Patient II-1 of Family 2 (E). Patients IV-2, IV-3 of Family 1, and II-1 of Family 2 showing ring scotomas in both eyes. Patient III-1 of Family 1 had normal visual fields. L, left eye; R, right eye. Patients are described in detail in Report of Cases.

## Discussion

Choroideremia is an X-linked disorder that is characterized by progressive degeneration of choroid, retina, and RPE, progressive visual field loss, and a reduction of visual acuity at the late stage. The fundus at the early stage of choroideremia shows areas of RPE disruption. With progression of the choroideremia, there is severe chorioretinal atrophy, loss of choriocapillaries, and finally bare sclera.

Positional cloning and the screening of cDNA library were performed to identify the entire coding

region of the *CHM* gene, which permitted the identification of the causative mutations for patients with choroideremia.[1–4]

The *CHM* gene encoded the Rab escort protein-1 (Rep-1), and Rep-1 presents Rab-proteins to the catalytic site of the enzymes. This adds geranylgeranyl groups to cysteines of the carboxy-terminus of Rab proteins. These proteins play an important role in intracellular vesicular transport.

To date, nonsense, frameshift, and splice site mutations in the *CHM* gene have been identified.[1–16] For Japanese patients with choroideremia, 15 kinds of mutations have been reported.[13–15] We found a novel 402delT mutation and the 555–556delAG mutation in the two Japanese families with choroideremia. These mutations caused a frameshift and premature termination at codon 125 and 182, and if translated, the mutated CHM protein would not be functional.

The severity of the clinical features produced by these mutations was variable. Thus, Patient IV-3 of Family 1 at the early stage of choroideremia at 23 years of age showed only mottled appearance of the RPE, and the characteristic severe chorioretinal atrophy was not present. However, Patient II-1 of Family 2, who had the 555–556delAG mutation and was 24 years old, showed marked chorioretinal atrophy and nonrecordable ERGs. It is not known how the different mutations alter the severity or phenotype of choroideremia. More cases associated with mutations in the *CHM* gene resulting in nonsense mutation, frameshift mutations, and splice site mutations are needed to understand the mechanism of clinical variability. In addition, additional cases must be studied to offer genetic counseling as requested by Family 1. From a clinical point of view, further correlations between specific mutations and their phenotypes are needed to augment our understanding of the molecular mechanism of diseases and also for diagnosis and prognosis.

**Key words:** *CHM* gene, choroideremia, clinical variability, mutation, x-linked.

## References

1. Cremers FP, van de Pol DJ, van Kerkhoff LP, et al. Cloning of a gene that is rearranged in patients with choroideremia. Nature 1990;347:674–677.
2. Merry DE, Yadvish KN, Landers JE, Lewis RA, Nussbaum RL. Isolation of a candidate gene for the human chorioretinal dystrophy choroideremia. Am J Hum Genet 1991;S413.
3. Merry DE, Janne PA, Landers JE, Lewis RA, Nussbaum RL. Isolation of a candidate gene for choroideremia. Proc Natl Acad Sci USA 1992;89:2135–2139.
4. van Bokhoven H, van den Hurk JA, Bogerd L, et al. Cloning and characterization of the human choroideremia gene. Hum Mol Genet 1994;3:1041–1046.
5. Sankila EM, Tolvanen R, van den Hurk JA, et al. Aberrant splicing of the CHM gene is a significant cause of choroideremia. Nat Genet 1992;1:109–113.
6. van Bokhoven H, Schwartz M, Andreasson S, et al. Mutation spectrum in the CHM gene of Danish and Swedish choroideremia patients. Hum Mol Genet 1994;3:1047–1051.
7. van den Hurk JA, van de Pol TJ, Molloy CM, et al. Detection and characterization of point mutations in the choroideremia candidate gene by PCR-SSCP analysis and direct DNA sequencing. Am J Hum Genet 1992;50:1195–1202.
8. Available at: www.retina.international.org.
9. Ponjavic V, Abrahamson M, Andreasson S, et al. Phenotype variations within a choroideremia family lacking the entire CHM gene. Ophthalmic Genet 1995;16:143–150.
10. Forsythe P, Maguire A, Fujita R, et al. A carboxy-terminal truncation of 99 amino acids resulting from a novel mutation (Arg555->stop) in the *CHM* gene leads to choroideremia. Exp Eye Res 1997;64:487–490.
11. van den Hurk JA, Schwartz M, van Bokhoven H, et al. Molecular basis of choroideremia (CHM): mutations involving the Rab escort protein-1 (REP-1) gene. Hum Mutat 1997; 9:110–117.
12. Hotta Y, Fujiki K, Hayakawa M, et al. A hemizygous A to CC base change of the CHM gene causing choroideremia associated with pinealoma. Graefes Arch Clin Exp Ophthalmol 1997;235:653–655.
13. Fujiki K, Hotta Y, Hayakawa M, et al. REP-1 gene mutations in Japanese patients with choroideremia. Graefes Arch Clin Exp Ophthalmol 1999;237:735–740.
14. Hayakawa M, Fujiki K, Hotta Y, et al. Visual impairment and REP-1 gene mutations in Japanese choroideremia patients. Ophthalmic Genet 1999;20:107–115.
15. Ohba N. Introduction to genetics in ophthalmology, value of family studies. Jpn J Ophthalmol 2000;44:320–321.
16. McTaggart KE, Tran M, Mah DY, et al. Mutational analysis of patients with the diagnosis of choroideremia. Hum Mutat 2002;20:189–196.
17. Marmor MF, Arden GB, Nilson SEG, Zrenner E. Standard for clinical electroretinography. Arch Ophthalmol 1989;107: 816–819.
18. Nakazawa M, Kikawa-Araki E, Shiono T, Tamai M. Analysis of rhodopsin gene in patients with retinitis pigmentosa using allele-specific polymerase chain reaction. Jpn J Ophthalmol 1991;35:386–393.